Advances in Aircraft and Spacecraft Science, *Vol. 12, No. 4 (2025) 367-385*
https://doi.org/10.12989/aas.2025.12.4.367

Investigating interfacial stresses and bending behavior in beams strengthened with bonded prestressed FRP plates

Abdelghani Brahimi*[1,2], Boucif Guenaneche[3], Okkacha Youb[4], Sidi Mohamed Bennaceur[1,2] and Khaled Amara[3,5]

[1]*Department of Civil Engineering, Faculty of Science and Technology, University of Naama, 45000, Algeria*
[2]*Artificial Intelligence Laboratory for Mechanical and Civil Structures, and Soil, University of Naama, 45000, Algeria*
[3]*Department of Civil Engineering, Faculty of Science and Technology, University of Ain Temouchent, 46000, Algeria*
[4]*Scientific and Technical Research Centre on Arid Regions (CRSTRA), Omar el Bernaoui, BP 1682 ,07000 Biskra, Algeria*
[5]*Engineering and Sustainable Development Laboratory, Ain Temouchent, 46000, Algeria*

(Received February 6, 2025, Revised July 27, 2025, Accepted September 26, 2025)

Abstract. In the present work, we present an explicit analytical solution for calculating the flexural and interfacial behavior of beams strengthened by prestressed bonded plates. Unlike existing approaches, our method comprehensively integrates shear-lag deformations from both the beam and the plate, thus providing a more accurate prediction of critical interfacial stresses and overall composite behavior. A parametric analysis was conducted to examine how variations in parameters such as prestress force and the geometric and mechanical characteristics of the reinforcement plate impact the behavior of the interface. These variations were found to significantly influence the maximum shear and normal stress within the composite element.

Keywords: bending; interfacial stresses; plate prestressed; shear deformation; strengthening

1. Introduction

The plate bonding technique serves to enhance the strength and stiffness or to repair existing reinforced concrete structures. This method is crucial for extending the service life of aging infrastructure and improving the resilience of structures against increased loading demands. Composite fiber reinforced plastic (FRP) has gained popularity due to its effectiveness and simplicity in this regard. The lightweight, high-strength, and corrosion-resistant properties of FRP make it an ideal material for external bonding applications.

Accurate prediction of interfacial stresses at the bondline is paramount for the safe and efficient design of such retrofitted structures. Several studies, including those conducted by Vilnay (1988), Roberts (1989), Roberts *et al.* (1989), Malek *et al.* (1994), Robinovitch *et al.* (2000), Ye (2001), Smith *et al.* (2001), Barnes *et al.* (2001), Stratford *et al.* (2006), Benyoucef *et al.* (2006), Tounsi *et al.* (2007), Bouazaoui (2008) have focused on predicting interfacial stresses. Understanding these

*Corresponding author, Ph.D., E-mail: brahimiabdelghani@cuniv-naama.dz

http://www.techno-press.org/aas/8 ISSN: 2287-528X (Print), 2287-5271 (Online)

stresses is key to preventing premature debonding failures, which can significantly compromise the integrity of the strengthened element.

Additionally, there has been significant progress in developing closed-form solutions for analyzing interfacial stresses in beams bonded with steel or FRP plates. As early as Taljsten (1997), valuable insights into stress transfer mechanisms were being provided. Building on this foundation, Rabinovich *et al.* (2000) introduced a higher-order analysis treating the adhesive layer as an elastic medium with minimal longitudinal stiffness. This approach resulted in predicting uniform shear stresses and linearly varying normal stresses within the adhesive layer while satisfying stress-free boundary conditions, thereby addressing some limitations of earlier, simpler models.

Further advancements in understanding interfacial stresses continued into the early 2000s. The approach proposed by Smith *et al.* (2001) stands out as widely applicable and accurate, particularly when considering the flexural stiffness of the bonded plate, which allows for a more realistic representation of the composite action. Rabinovich *et al.* (2001) delved into uneven adhesive layer effects and material nonlinearity, while Shen *et al.* (2001) offered an alternative analytical complementary energy approach. These concurrent studies highlight the complexity and multi-faceted nature of interfacial behavior. Following these, Smith *et al.* (2002), Tounsi (2006) also contributed significantly to the development of closed-form solutions.

More recently, the focus has expanded to encompass additional factors. Works by Benachour *et al.* (2008), Ghafoori (2013) provided solutions for interfacial stresses in steel beams strengthened by prestressed bonded FRP plates, showcasing the versatility of the technique.

Parallel to these analytical advancements, recent numerical studies have greatly enhanced our understanding. Bouakaz *et al.* (2014), Krour *et al.* (2014) were among the first in this wave of detailed numerical investigations. Subsequent works by Touati *et al.* (2015), Hadji *et al.* (2016), Elamary *et al.* (2016), Daouadji (2017) have further delved into various parameters to estimate interfacial stress distributions in beams reinforced with composite plates. These numerical investigations complement analytical models by allowing for the analysis of more complex geometries, material behaviors, and loading conditions, providing a comprehensive view of the interface. Lastly, Antar *et al.* (2019, 2024) presented the hygro-thermal effect on the interfacial shear and normal stresses, demonstrating the importance of environmental factors on long-term performance.

In our paper, we present a detailed analytical method that considers shear-lag deformations in both the beam to analyze the flexural and interfacial behavior of beams enhanced with prestressed bonded plates. This refined approach provides a more accurate representation of the stress and strain distribution, particularly near the ends of the bonded plates where stress concentrations are highest. It contributes to improving existing methodologies and advancing our understanding of structural enhancements using these techniques, ultimately leading to more robust and reliable design practices.

2. Theoretical modelling

As shown in Fig. 1, a concrete beam (Adherend 1) strengthened by FRP plate (Adherend 2) and bounded by an adhesive layer is considered. This beam is simply supported reinforced beam and subjected to a uniformdistributed load. Geometry and cross-sections are shown in Fig. 1.

The following assumptions are used:

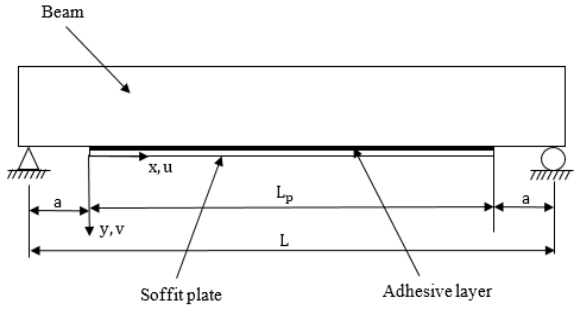

Fig. 1 Soffit-plated beam

- The materials concrete beam, FRP plate and adhesive are linear elastic.
- Shear and normal stresses in the adhesive layer are constant across its thickness.
- The curvature in the beam and the plate are same.

2.1 Governing equations

The total longitudinal deformations in the upper and lower parts of the adhesive layer $\varepsilon_i(x)$ are obtained from axial deformations $\varepsilon_i^N(x)$ and deformations due to bending moments $\varepsilon_i^M(x)$.

$$\varepsilon_i(x) = \frac{du_i(x)}{dx} = \varepsilon_i^N(x) + \varepsilon_i^M(x) \quad i = 1;2 \tag{1}$$

$$\varepsilon_1(x) = \frac{du_1(x)}{dx} = \varepsilon_1^N(x) + \varepsilon_1^M(x) \tag{2}$$

$$\varepsilon_2(x) = \frac{du_2(x)}{dx} = \varepsilon_2^N(x) + \varepsilon_2^M(x) \tag{3}$$

The longitudinal deformations of the beam and the FRP reinforcement plate are noted by $\varepsilon_1^N(x)$ and $\varepsilon_2^N(x)$ at the adhesive interface. They are due to longitudinal forces $N_i(x)$.

Due to the fact that the shear stresses are null at the upper and lower free edges of the reinforced beam, using the method developed by Tounsi *et al.* (2006), and we assume a parabolic variation of the displacement $U_i^N(x,y)$ of the fibers through the thickness of the plate and the beam and after different algebraic operations, we obtain the axial deformations $\varepsilon_i^N(x)$ which take into account shear deformations (shear-lag) at the lower edges and upper respectively of the beam and the plate.

The Longitudinal displacements in the two adherents $U_1^N(x,y)$ and $U_2^N(x,y)$ are represented by a parabolic function of second degree in y for the adherent and *y*' for the adherent 2

$$U_1^N(x,y) = A_1(x)\cdot y^3 + B_1(x)\cdot y + C_1(x) \tag{4}$$

$$U_2^N(x,y') = A_2(x)\cdot y'^3 + B_2(x)\cdot y' + C_2(x) \tag{5}$$

The shear stresses in the two adherents are given by

$$\sigma_{xy}(1) = G_1 \cdot \gamma_{xy}(1) \tag{6}$$

$$\sigma_{xy}(2) = G_2 \cdot \gamma_{xy'}(2) \tag{7}$$

The shear deformations of the adhesive are expressed as follows

$$\gamma_{xy}(i) = \frac{dU_i^N}{dy} + \frac{dW_i^N}{dx} \; ; \; i = 1{,}2 \tag{8}$$

Where G_1 and G_2 are the transverse shear modulus of adherent 1 and 2, respectively.

By neglecting the variations in transverse displacement W_i^N (induced by longitudinal forces $N_i(x)$), with the longitudinal coordinate x

$$\gamma_{xy}(i) = \frac{\partial W_i^N}{\partial x} \approx 0 \tag{9}$$

$$\gamma_{xy}(i) = \frac{dU_i^N}{dy} \tag{10}$$

$$\gamma_{\mathrm{xy}}(\mathrm{i}) = \; 3 \cdot A_i(x) \cdot y^2 + B_i(x) \; ; \; i = 1{,}2 \tag{11}$$

$$\sigma_{\mathrm{xy}}(1) = \mathrm{G_1} \cdot 3 \cdot A_i(x) \cdot y^2 + B_i(x) \; ; \; i = 1{,}2 \tag{12}$$

The shear stresses must satisfy the following conditions

$$\sigma_{xy(1)}(x, t_1) = \sigma_{xy'(2)}(x, 0) = \tau(x) = \tau_a \tag{13}$$

$$\sigma_{xy(1)}(x, 0) = \sigma_{xy'}(x, t_2) = 0 \tag{14}$$

Where t_1 and t_2 are respectively the thickness values of adherents 1 and 2. Condition (13) arises from continuity and the assumption of uniform shear stresses across the thickness of the adhesive. Condition (14) states that there is no shear stress at the top surface of adherent 1 (i.e., at y=0) and at the bottom surface of adherent 2 (i.e., at y'=t2). These conditions lead to the following expressions

$$\sigma_{xy}(1) = \frac{\tau(x)}{t_1^2} \cdot y^2 \tag{15}$$

$$\sigma_{xy'}(2) = (1 - \frac{{y'}^2}{t_2^2}) \cdot \tau(x) \tag{16}$$

Then, with a linear material constitutive relation, the shear strains of the two adherents, γ_1 for adherent 1 and γ_2 for adherent 2, are expressed as follows

$$\gamma_{xy}(1) = \gamma_1 = \frac{\tau_a}{G_1 \cdot t_1^2} \cdot y^2 \tag{17}$$

$$\gamma_{xy'}(2) = \gamma_2 = \frac{\tau_a}{G_2} \cdot (1 - \frac{{y'}^2}{t_2^2}) \tag{18}$$

The functions of longitudinal displacement, U_1^N for the adherent 1 and U_2^N for the adherent 2, due to longitudinal forces, are given by

$$U_1^N(y) = U_1^N(0) + \int_0^y \gamma_1(y)dy = U_1^N(0) + \frac{\tau_a}{3 \cdot G_1 \cdot t_1^2} \cdot y^3 \tag{19}$$

$$U_2^N(y') = u_2^N + \int_0^{y'} \gamma_2(y')dy' = u_2^N + \frac{\tau_a}{G_2} \cdot \left(y' - \frac{{y'}^3}{3 \cdot t_2^2}\right) \tag{20}$$

$U_1^N(0)$ represents the displacement on the upper surface of adherent 1 (due to longitudinal forces $N_1(x)$), and U_2^N represents the adhesive displacement induced by the longitudinal force $N_2(x)$ at the interface between the adhesive and the adherent 2. The displacement of fibers at the lower base of adherent 1 u_1^N is given by the following expression

$$u_1^N = U_1^N(y = t_1) = U_1^N(0) + \frac{\tau_a \cdot t_1}{3 \cdot G_1} \tag{21}$$

Eqs. (17) and (18) can be rewritten as follows

$$U_1^N(y) = u_1^N + \frac{\tau_a}{3 \cdot G_1 \cdot t_1^2} \cdot y^3 - \frac{\tau_a \cdot t_1}{3 \cdot G_1} \tag{22}$$

$$U_2^N(y') = u_2^N - \frac{\tau_a}{3 \cdot G_2 \cdot t_2^2} \cdot y'^3 + \frac{\tau_a \cdot y'}{G_2} \tag{23}$$

The resulting longitudinal force ΔN_2, for the lower adherent is

$$\Delta N_2(x) = N_2(x) - N_0 \tag{24}$$

$$\Delta N_2(x) = b_2 \cdot \int_0^{t_2} \sigma_2^N(y')dy' \tag{25}$$

In which ΔN_2 represents the result of the longitudinal normal stresses for adherent 2. By substituting Eq. (21) into Eq. (22), and expanding the expression for the constraints, we can write

$$\Delta N_2(x) = E_2 \cdot A_2 \cdot \left\{\frac{du_2^N(x)}{dx} + \frac{5 \cdot t_2}{12 \cdot G_2} \cdot \frac{d\tau(x)}{dx}\right\} \tag{26}$$

$$A_2 = b_2 \cdot t_2 \tag{27}$$

La the longitudinal deformation of the plate induced by the longitudinal forces $N_2(x)$ can be expressed as follows

$$\epsilon_2^N(x) = \frac{du_2^N(x)}{dx} = \frac{\Delta N_2(x)}{E_2 \cdot A_2} - \frac{5 \cdot t_2}{12 \cdot G_2} \cdot \frac{d\tau(x)}{dx} \tag{28}$$

The longitudinal equation for longitudinal deformation of the plate can be expressed as follows

$$\varepsilon_2(x) = \frac{du_2(x)}{dx} = -\frac{y_2 \cdot M_2(x)}{E_2 \cdot I_2} + \frac{\Delta N_2(x)}{E_2 \cdot A_2} - \frac{5 \cdot t_2}{12 \cdot G_2} \cdot \frac{d\tau(x)}{dx} \tag{29}$$

The resulting longitudinal force $N_1(x)$ for the upper adherent is given by

$$N_1(x) = b_1 \cdot \int_0^{t_0} \sigma_1^N(y)dy + b_0 \cdot \int_{t_0}^{t_1 - t_0} \sigma_1^N(y)dy + b_1 \cdot \int_{t_1 - t_0}^{t_1} \sigma_1^N(y)dy \tag{30}$$

$$N_1(x) = b_1 \cdot \int_0^{t_0} E_1 \cdot \frac{dU_1^N(y)}{dx} \cdot dy + b_0 \cdot \int_{t_0}^{t_1 - t_0} E_1 \cdot \frac{dU_1^N(y)}{dx} \cdot dy + b_1 \cdot \int_{t_1 - t_0}^{t_1} E_1 \cdot \frac{dU_1^N(y)}{dx} \cdot dy \tag{31}$$

After expansion and arrangement, Eq. (31) can be written as follows

$$N_1(x) = E_1 \cdot A_1 \cdot \left\{\frac{du_1^N}{dx} + \frac{1}{12 \cdot G_1 \cdot t_1^2} \cdot \left[b_1 \cdot \left(\frac{-t_0^4 + 8 \cdot t_1^3 \cdot t_0 - t_1^4 + (t_1 - t_0)^4}{A_1}\right) + b_0 \cdot \left(\frac{4 \cdot t_1^3 \cdot (t_1 - 2 \cdot t_0) - (t_1 - t_0)^4 + t_0^4}{A_1}\right) \frac{d\tau(x)}{dx}\right]\right\} \tag{32}$$

$$A_1 = 2 \cdot b_1 \cdot t_0 + b_0 \cdot (t_1 - 2 \cdot t_0) \tag{33}$$

Eq. (32) leads to the longitudinal deformation of the beam induced by the longitudinal force

$N_1(x)$.

$$\epsilon_1^N(x) = \frac{du_1^N(x)}{dx} = \frac{N_1(x)}{E_1 \cdot A_1} - \frac{1}{12 \cdot G_1 \cdot t_1^2} \cdot \left[b_1 \cdot \left(\frac{-t_0^4 + 8 \cdot t_1^3 \cdot t_0 - t_1^4 + (t_1 - t_0)^4}{A_1} \right) + b_0 \cdot \left(\frac{4 \cdot t_1^3 \cdot (t_1 - 2 \cdot t_0) - (t_1 - t_0)^4 + t_0^4}{A_1} \right) \right] \frac{d\tau(x)}{dx} \tag{34}$$

$$\varepsilon_1(x) = \frac{du_1(x)}{dx} = \frac{y_1 \cdot M_1(x)}{E_1 \cdot I_1} - \frac{du_1^N(x)}{dx} \tag{35}$$

The cross sections of adherent 1 and 2 are represented by A_1 and A_2, respectively. By substituting Eq. (31) into Eq. (35), the total deformation can be expressed as follows

$$\varepsilon_1(x) = \frac{du_1(x)}{dx} = \frac{y_1 \cdot M_1(x)}{E_1 \cdot I_1} - \frac{N_1(x)}{E_1 \cdot A_1} + \frac{1}{12 \cdot G_1 \cdot t_1^2} \cdot \left[b_1 \cdot \left(\frac{-t_0^4 + 8 \cdot t_1^3 \cdot t_0 - t_1^4 + (t_1 - t_0)^4}{A_1} \right) + b_0 \cdot \left(\frac{4 \cdot t_1^3 \cdot (t_1 - 2 \cdot t_0) - (t_1 - t_0)^4 + t_0^4}{A_1} \right) \right] \frac{d\tau(x)}{dx} \tag{36}$$

The expression for the total deformation of the beam can be rewritten as follows

$$\varepsilon_1(x) = \frac{du_1(x)}{dx} = \frac{y_1 \cdot M_1(x)}{E_1 \cdot I_1} - \frac{N_1(x)}{E_1 \cdot A_1} + \frac{t_1}{4 \cdot G_1} \cdot \xi \cdot \frac{d\tau(x)}{dx} \tag{37}$$

$$\xi = \frac{1}{3 \cdot A_1 \cdot t_1^3} \cdot [b_1 \cdot (-t_0^4 + 8 \cdot t_1^3 \cdot t_0 - t_1^4 + (t_1 - t_0)^4) + b_0 \cdot (4 \cdot t_1^3 \cdot (t_1 - 2 \cdot t_0) - (t_1 - t_0)^4 + t_0^4)] \tag{38}$$

The shear stress in the adhesive layer can be expressed as follows

$$\tau(x) = K_s \cdot \left(u_2(x) - u_1(x) \right) \tag{39}$$

$$K_s = \frac{G_a}{t_a} \tag{40}$$

$$\frac{d\tau(x)}{dx} = K_s \cdot \left(\frac{du_2^N(x)}{dx} - \frac{du_1(x)}{dx} \right) \tag{41}$$

By considering the balance of the axial forces of the infinitesimal element, we obtain the following expressions

$$\frac{dN_i(x)}{dx} = b_2 \cdot \tau(x) \ , i = 1,2 \tag{42}$$

After integration we have

$$N_i(x) = N(x) = b_2 \cdot \int_0^x \tau(x) \cdot dx \ , i = 1,2 \tag{43}$$

Where b_2 is the width of the reinforcement plate.

From the vertical balance of the infinitesimal element, the following relations are obtained

$$\frac{dV_i(x)}{dx} = (-1)^i \cdot [q_i + b_2 \cdot \sigma(x)] \, , i = 1, q_i = q; i = 2, q_i = 0 \tag{44}$$

$$\frac{dM_i(x)}{dx} = V_i(x) - b_2 \cdot y_i \cdot \tau(x), \quad i = 1,2 \tag{45}$$

$$M_1(x) = R \cdot M_2(x) \tag{46}$$

Where

$$R = \frac{E_1 \cdot I_1}{E_2 \cdot 2} \tag{47}$$

The balance of the moments of the infinitesimal element of the reinforced beam (Fig. 1) allows us to obtain the total moment $M_T(x)$ as follows

$$M_T(x) = M_1(x) + M_2(x) + N(x) \cdot (y_1 + y_2 + t_a) \tag{48}$$

By introducing Eqs. (43) and (46) into Eq. (48), we obtain the relations of the bending moments of each adherent.

$$M_i(x) = \frac{E_i \cdot I_i}{(EI)_t} \cdot (M_T(x) - b_2 \cdot \int_0^x \tau(x) \cdot (y_1 + y_2 + t_a) dx \, , i = 1{,}2 \tag{49}$$

The expression of the shear force of each adherent is obtained by deriving the previous equation

$$V_i(x) = \frac{dM_i(x)}{dx} = \frac{E_i \cdot I_i}{(EI)_t} \cdot [V_T(x) - b_2 \cdot \tau(x) \cdot (y_1 + y_2 + t_a)] \, , i = 1{,}2 \tag{50}$$

$$\frac{d\tau(x)}{dx} = \frac{1}{K_1} \cdot \left\{ -\frac{y_2}{E_2 \cdot I_2} \cdot M_2(x) + \frac{\Delta N_2(x)}{E_2 \cdot A_2} - \frac{y_1}{E_1 \cdot I_1} \cdot M_1(x) + \frac{N_1(x)}{E_1 \cdot A_1} \right\} \tag{51}$$

$$K_1 = \frac{t_a}{G_a} + \frac{t_1}{4 \cdot G_1} \cdot \xi + \frac{5 \cdot t_2}{12 \cdot G_2} \tag{52}$$

By deriving Eq. (51) following x we obtain

$$\frac{d^2\tau(x)}{dx^2} = \frac{1}{K_1} \cdot \left\{ -\frac{y_2}{E_2 \cdot I_2} \cdot \frac{dM_2(x)}{dx} + \frac{1}{E_2 \cdot A_2} \cdot \frac{d\Delta N_2(x)}{dx} - \frac{y_1}{E_1 \cdot I_1} \cdot \frac{dM_1(x)}{dx} + \frac{1}{E_1 \cdot A_1} \cdot \frac{dN_1(x)}{dx} \right\} \tag{53}$$

$$\begin{aligned} \frac{d^2\tau(x)}{dx^2} = \frac{1}{K_1} \cdot \Bigg[& -\frac{y_2}{E_2 \cdot I_2} \cdot \frac{1}{R+1} \cdot \{V_T(x) - b_2 \cdot \tau(x) \cdot (y_1 + y_2 + t_a)\} + \frac{1}{E_2 \cdot A_2} \cdot \frac{d(\Delta N_2(x))}{dx} - \frac{y_1}{E_1 \cdot I_1} \cdot \\ & \frac{R}{R+1} \cdot \{V_T(x) - b_2 \cdot \tau(x) \cdot (y_1 + y_2 + t_a)\} + \frac{1}{E_1 \cdot A_1} \cdot \frac{dN_1(x)}{dx} \Bigg] \end{aligned} \tag{54}$$

Substituting the bending moment Eq. (49) and the axial force eEq. (43) into equation provides the overall differential equation for the shear stress.

$$\frac{d^2\tau(x)}{dx^2} - b_2 \cdot \frac{1}{K_1} \cdot \left[\frac{1}{E_1 \cdot A_1} + \frac{1}{E_2 \cdot A_2} + \frac{(y_1+y_2) \cdot (y_1+y_2+t_a)}{(EI)_t} \right] \cdot \tau(x) + \frac{1}{K_1} \cdot \frac{(y_1+y_2)}{(EI)_t} \cdot V_T(x) = 0 \tag{55a}$$

$$\frac{d^2\tau(x)}{dx^2} - \alpha_1 \cdot \tau(x) + \beta_1 \cdot V_T(x) = 0 \tag{55b}$$

$$\alpha_1 = \frac{b_2}{K_1} \cdot \left[\frac{1}{E_1 \cdot A_1} + \frac{1}{E_2 \cdot A_2} + \frac{(y_1+y_2) \cdot (y_1+y_2+t_a)}{(EI)_t} \right] \qquad \beta_1 = \frac{1}{K_1} \cdot \frac{(y_1+y_2)}{(EI)_t} \tag{55c}$$

$$\lambda^2 = \alpha_1 = \frac{b_2}{K_1} \cdot \left[\frac{1}{E_1 \cdot A_1} + \frac{1}{E_2 \cdot A_2} + \frac{(y_1+y_2) \cdot (y_1+y_2+t_a)}{(EI)_t} \right] \tag{55d}$$

$$m_1 = \frac{\beta_1}{\lambda^2} \tag{55e}$$

$$\beta_1 = m_1 \cdot \lambda^2 \tag{55f}$$

The normal stress is expressed by the following equation

$$\sigma(x) = \mathrm{K_n} \cdot [w_2(\mathrm{x}) - w(\mathrm{x})] \tag{56}$$

$w_1(x)$ and $w_2(x)$ are the normal displacements of adherent 1 and 2, respectively.

By deriving Eq. (56) twice, we obtain

$$\frac{d^2\sigma(x)}{dx^2} = K_n \cdot \left(\frac{d^2w_2(x)}{dx^2} - \frac{d^2w_1(x)}{dx^2}\right) \tag{58}$$

Based on the relations of the moment curvatures of the beams and plates, we have the following expressions

$$\frac{d^2w_1(x)}{dx^2} = -\frac{1}{E_1 \cdot I_1} M_1(x) \tag{59}$$

$$\frac{d^2w_2(x)}{dx^2} = -\frac{1}{E_2 \cdot I_2} M_2(x) \tag{60}$$

By replacing expression (45) in the first derivative of Eq. (60) with respect to x, we have

$$\frac{d^3w_1(x)}{dx^3} = -\frac{1}{E_1 \cdot I_1} \cdot \frac{dM_1(x)}{dx} = -\frac{1}{E_1 \cdot I_1} \cdot [V_1(x) - b_2 \cdot y_1 \cdot \tau(x)] \tag{61}$$

By replacing Eqs. (45) and (46) in the fourth derivative of Eqs. (59) and (60), the differential equations of the vertical deformation of adherent 1 $w_1(x)$ and the vertical deformation of adherent 2 of the beam $w_2(x)$, are given as follows

$$\frac{d^4w_1(x)}{dx^4} = -\frac{1}{E_1 \cdot I_1} \cdot \left[\frac{dV_1(x)}{dx} - b_2 \cdot y_1 \cdot \frac{d\tau(x)}{dx}\right] = -\frac{1}{E_1 \cdot I_1} \cdot \left[-b_2 \cdot \sigma(x) - q - b_2 \cdot y_1 \cdot \frac{d\tau(x)}{dx}\right] \tag{62}$$

$$\frac{d^4w_1(x)}{dx^4} = \frac{1}{E_1 \cdot I_1} \cdot \sigma(x) + \frac{b_2 \cdot y_1}{E_1 \cdot I_1} \cdot \frac{d\tau(x)}{dx} + \frac{q}{E_1 \cdot I_1} \tag{63}$$

$$\frac{d^3w_2(x)}{dx^3} = -\frac{1}{E_2 \cdot 2} \cdot \frac{dM_2(x)}{dx} = -\frac{1}{E_2 \cdot I_2} \cdot [V_2(x) - b_2 \cdot y_2 \cdot \tau(x)] \tag{64}$$

$$\frac{d^4w_2(x)}{dx^4} = -\frac{b_2}{E_2 \cdot I_2} \cdot \sigma(x) + \frac{b_2 \cdot y_2}{E_2 \cdot I_2} \cdot \frac{d\tau(x)}{dx} \tag{65}$$

$$\frac{d^4\sigma(x)}{dx^4} = \frac{E_a}{t_a} \cdot \left[\frac{d^4w_2(x)}{dx^4} - \frac{d^4w_1(x)}{dx^4}\right] \tag{66}$$

Substituting Eqs. (63) and (65) into Eq. (58), gives us the differential equation of the normal stress.

$$\frac{d^4\sigma(x)}{dx^4} = \frac{E_a}{t_a} \cdot \left[-\frac{b_2}{E_2 \cdot I_2} \cdot \sigma(x) + \frac{b_2 \cdot y_2}{E_2 \cdot I_2} \cdot \frac{d\tau(x)}{dx} - \frac{b_2}{E_1 \cdot I_1} \cdot \sigma(x) - \frac{b_2 \cdot y_1}{E_1 \cdot I_1} \cdot \frac{d\tau(x)}{dx} - \frac{q}{E_1 \cdot I_1}\right] \tag{67}$$

After rearrangement of Eq. (67) we have

$$\frac{d^4\sigma(x)}{dx^4} + \frac{E_a}{t_a} \cdot b_2 \cdot \left(\frac{1}{E_1 \cdot I_1} + \frac{1}{E_2 \cdot I_2}\right) \cdot \sigma(x) + \frac{E_a}{t_a} \cdot b_2 \cdot \left(\frac{y_1}{E_1 \cdot I_1} - \frac{y_2}{E_2 \cdot I_2}\right) \cdot \frac{d\tau(x)}{dx} + \frac{q}{E_1 \cdot I_1} \cdot \frac{E_a}{t_a} \tag{68}$$

The general solution of this fourth order differential equation is

$$\sigma(x) = e^{-\beta \cdot x} \cdot [C_1 \cdot \cos(\beta \cdot x) + C_2 \cdot \sin(\beta x)] + e^{\beta \cdot x} \cdot [C_3 \cdot \cos(\beta \cdot x) + C_4 \cdot \sin(\beta \cdot x)] - n_1 \cdot \frac{d\tau(x)}{dx} - n_2 \cdot q \tag{69}$$

C_3 and C_4 are the integration constants.

For the large values of x, it is assumed that the normal stress tends towards zero and, therefore, C_3=C_4=0. The general solution becomes.

$$\sigma(x) = e^{-\beta \cdot x} \cdot [C_1 \cdot \cos(\beta \cdot x) + C_2 \cdot \sin(\beta \cdot x) +] - n_1 \cdot \frac{d\tau(x)}{dx} - n_2 \cdot q \tag{70a}$$

$$\beta = \sqrt[4]{\frac{E_a \cdot b_2}{4 \cdot t_a} \cdot \left(\frac{1}{E_1 \cdot I_1} + \frac{1}{E_2 \cdot I_2}\right)} \tag{70b}$$

$$n_1 = \frac{y_1 \cdot E_2 \cdot I_2 - y_2 E_1 \cdot I_1}{E_1 \cdot I_1 + E_2 \cdot I_2} \tag{70c}$$

$$n_2 = \frac{E_2 \cdot I_2}{b_2 \cdot (E_1 \cdot I_1 + E_2 \cdot I_2)} \tag{70d}$$

The general solution of Eq. (55b) is given by

$$\tau(x) = B_1 \cdot \cosh(\lambda \cdot x) + B_2 \cdot \sinh(\lambda \cdot x) + m_1 \cdot V_T(x) \tag{71}$$

The integration constants B_1 and B_2 will be determined depending on the type of loading.

where $\lambda^2 = \alpha_1$ et $m_1 = \frac{\beta_1}{\lambda^2}$

Substituting the expression for the shear force in a simply supported beam subjected to a uniformly distributed load into Eq. (71). The general solution of the interfacial shear stresses for this load case can be expressed as follows

$$\tau(x) = B_1 \cdot \cosh(\lambda \cdot x) + B_2 \cdot \sinh(\lambda \cdot x) + m_1 \cdot q \cdot (\frac{L}{2} - a - x) \quad 0 \leq x \leq \frac{L_p}{2} \tag{72}$$

where q is the uniformly distributed load and x, a, L and L_P are defined in Fig. 1. The integration constants must be determined by respecting appropriate boundary conditions.

The boundary conditions of the distributed loads are formulated as follows

$$M_2(0) = N_2(0) = N_1(0) = 0\ ,\ M_1(0) = M_T(0) \text{ and } \frac{dV_T(0)}{dx} = -q \tag{73}$$

With: $\tau(L_p/2) = 0$

The derivative of the shear stress expression is given by the following equation

$$\frac{d\tau(x)}{dx} = \lambda \cdot B_1 \cdot \sinh(\lambda \cdot x) + \lambda \cdot B_2 \cdot \cosh(\lambda \cdot x) - m_1 \cdot q \tag{74}$$

By applying the boundary conditions defined by the Eq. (73) to Eqs. (72) and (74) we have the expressions of the integration constants B_2 and B_1

$$B_2 = \frac{m_1 \cdot q}{\lambda} - \frac{1}{\lambda} \cdot \frac{1}{K_1} \cdot \left[\frac{y_1}{E_1 \cdot I_1} \cdot M_T(0) + \frac{N_0}{E_2 \cdot A_2}\right] \tag{75a}$$

$$M_T(0) = \frac{q \cdot a}{2} \cdot (L - a) \tag{75b}$$

$$B_1 = -B_2 \cdot \tanh\left(\frac{\lambda \cdot L_P}{2}\right) \tag{75c}$$

For practical cases $\frac{\lambda \cdot L_P}{2} > 10$ and $tanh\left(\frac{\lambda \cdot L_P}{2}\right) \approx 1$ therefore, the expression for B_1 can be simplified to

$$B_1 = -B_2 \tag{76}$$

By replacing B_2 with in Eq. (76) we have

$$B_1 = -B_2 = -\frac{m_1 \cdot q}{\lambda} + \frac{1}{\lambda} \cdot \frac{1}{K_1} \cdot \left[\frac{y_1}{E_1 \cdot I_1} \cdot M_T(0) + \frac{N_0}{E_2 \cdot A_2}\right] \tag{77}$$

Substituting B_1 and B_2 into Eq. (72) gives the expression for the interfacial shear stress at any point.

$$\tau(x) = \left\{-\frac{m_1 \cdot q}{\lambda} + \frac{1}{\lambda . K_1} \cdot \left[\frac{y_1}{E_1 \cdot I_1} \cdot \left(\frac{q \cdot a}{2} \cdot (L-a)\right) + \frac{N_0}{E_2 \cdot A_2}\right]\right\} e^{-\lambda \cdot x} + m_1 \cdot q \cdot \left(\frac{L}{2} - a - x\right) \quad x \le L_p \quad (78)$$

Eq. (70a) has two unknowns C_1 and C_2 which can be determined using the appropriate boundary conditions. The first boundary condition comes from the null bending moment at the end of the FRP Plate. Substitution of Eq. (73) in the second derivative of Eq. (58) leads to the following relation

$$\frac{d^2\sigma(0)}{dx^2} = \frac{E_a}{t_a} \cdot \left(\frac{M_1(0)}{E_1 \cdot I_1} - \frac{M_2(0)}{E_2 \cdot I_2}\right) \quad (79)$$

At the end of the FRP plate, the boundary conditions are described as follows

$$N_1(0) = N_2(0) = M_2(0) = V_2(0) = 0\,, V_1(0) = V_T(0)\ and\ M_1(0) = M_T(0) \quad (80a)$$

$$V_T(0) = q \cdot \left(\frac{L}{2} - a\right)\ and\ \ M_T(0) = \frac{q}{2} \cdot a \cdot (L-a) \quad (80b)$$

The expression above can be written

$$\frac{d^2\sigma(0)}{dx^2} = \frac{E_a}{t_a} \cdot \frac{M_T(0)}{E_1 \cdot I_1} \quad (81)$$

The substitution of Eqs. (80a) and (80b) in the third derivative of Eq. (58) gives the following expression

$$\frac{d^3\sigma(0)}{dx^3} = \frac{E_a}{t_a} \cdot \left(\frac{V_1(0)}{E_1 \cdot I_1} - \frac{V_2(0)}{E_2 \cdot I_2}\right) - \frac{E_a}{t_a} \cdot \left(\frac{y_1}{E_1 \cdot I_1} - \frac{y_2}{E_2 \cdot I_2}\right) \cdot \tau(0) \quad (82)$$

Since the shear force is null at the end of the FRP plate $V_2(0)=0$, so , $V_1(0)=V_T(0)$, and hence the above relations can be expressed as follows

$$\frac{d^3\sigma(0)}{dx^3} = \frac{E_a}{t_a . E_1 \cdot I_1} \cdot V_T(0) - n_3 \cdot \tau(0) \quad (83)$$

Where

$$n_3 = \frac{E_a}{t_a} \cdot \left(\frac{y_1}{E_1 \cdot I_1} - \frac{y_2}{E_2 \cdot I_2}\right) \quad (84)$$

The second and third derivatives of the interface normal stress at the end of the FRP plate are given the following relations

$$\frac{d^2\sigma(0)}{dx^2} = -2 \cdot \beta^2 \cdot C_2 - n_1 \cdot \frac{d^3\tau(0)}{dx^3} - n_2 \cdot \frac{d^2 q}{dx^2} \quad (85)$$

$$\frac{d^3\sigma(0)}{dx^3} = 2 \cdot \beta^2 \cdot C_1 + 2 \cdot \beta^2 \cdot C_2 - n_1 \cdot \frac{d^4\tau(0)}{dx^4} - n_2 \cdot \frac{d^3 q}{dx^3} \quad (86)$$

The loading, considered in this work, is limited to a uniformly distributed load q, and therefore the second and higher order derivatives of q become zero (i.e., $dq/dx2=d3q/dx3=0$). Substituting Eqs. (82) and (83) into Eqs. (84) and (85), respectively, gives the expressions for the coefficients C_1 and C_2

$$C_1 = \frac{E_a}{2 \cdot t_a . \beta^3 \cdot E_1 \cdot I_1} \cdot [V_T(0) + \beta \cdot M_T(0)] - \frac{n_3}{2 \cdot \beta^3} \cdot \tau(0) + \frac{n_1}{2 \cdot \beta^3} \cdot \left(\frac{d^4\tau(0)}{dx^4} + \beta \cdot \frac{d^3\tau(0)}{dx^3}\right) \quad (87a)$$

$$C_2 = \frac{-E_a}{2 \cdot t_a \cdot \beta^2 \cdot E_1 \cdot I_1} \cdot M_T(0) - \frac{n_1}{2 \cdot \beta^2} \cdot \frac{d^3\tau(0)}{dx^3} \tag{87b}$$

Substituting C_1 and C_2 into Eq. (70a), the normal stress at the interface can be evaluated in terms of the bending moment $M_T(0)$ and the shear force $V_T(0)$ and is linked to any load case by its interface shear stress and its derivatives at the end of the FRP plate (i.e., $\tau(0)$,$\frac{d^3\tau_{(0)}}{dx^3}$, etc.).

2.2 Bending of beams reinforced by FRP plates

The equation for the variation of axial load varies along the FRP plate is obtained by substituting Eqs. (24), (43) and (48) into Eq. (51)

$$K_1 \cdot \frac{d\tau(x)}{dx} + \frac{(y_1+y_2)}{(EI)_t} \cdot M_T(x) + \frac{N_0}{E_2 \cdot A_2} = N(x) \cdot \left[\frac{1}{E_1 \cdot A_1} + \frac{1}{E_2 \cdot A_2} + \frac{(y_1+y_2)\cdot(y_1+y_2+t_a)}{(EI)_t}\right] \tag{88}$$

$$\frac{d\tau(x)}{dx} + \frac{1}{K_1} \cdot \frac{(y_1+y_2)}{(EI)_t} \cdot M_T(x) + \frac{1}{K_1} \cdot \frac{N_0}{E_2 \cdot A_2} = N(x) \cdot \frac{\lambda^2}{b_2} \tag{89a}$$

$$\frac{\lambda^2}{b_2} = \frac{1}{E_1 \cdot A_1} + \frac{1}{E_2 \cdot A_2} + \frac{(y_1+y_2)\cdot(y_1+y_2+t_a)}{(EI)_t} \tag{89b}$$

After rearranging Eq. (89a), the relations of the axial load $N(x)$ in the reinforcing plate is given as follows

$$N(x) = \frac{b_2}{\lambda^2} \cdot \left[\frac{d\tau(x)}{dx} + m_1 \cdot \lambda^2 \cdot M_T(x) + \frac{1}{K_1} \cdot \frac{N_0}{E_2 \cdot A_2}\right] \tag{90}$$

The bending behavior of the beam changes as it is reinforced by the FRP plate. Eq. (47) can be expressed in the following form

$$M_1(x) = \frac{E_1 \cdot I_1}{E_1 \cdot I_1 + E_2 \cdot I_2} \cdot \left(M_T(x) - N(x) \cdot (y_1 + y_2 + t_a)\right) \tag{91}$$

Substituting the above equation into Eq. (59) gives

$$\frac{d^2 w_1(\mathrm{x})}{dx^2} = -\frac{1}{E_1 \cdot I_1 + E_2 \cdot I_2} \cdot \left(M_T(x) - N(x) \cdot (y_1 + y_2 + t_a)\right) \tag{92}$$

where $N(x)$ is the axial force, which can be replaced by Eq. (90)

$$\frac{d^2 w_1(\mathrm{x})}{dx^2} = -\frac{1}{E_1 \cdot I_1 + E_2 \cdot I_2} \cdot \left(M_T(x) - \frac{b_2}{\lambda^2} \cdot \left[\frac{d\tau(x)}{dx} + m_1 \cdot \lambda^2 \cdot M_T(x) + \frac{1}{K_1} \cdot \frac{N_0}{E_2 \cdot A_2}\right] \cdot (y_1 + y_2 + t_a)\right) \tag{93}$$

Integrating the second order differential Eq. (92) with respect to x in the reinforced zone of the beam, we obtain the expression of the first order differential equation of the vertical deformation with a constant denoted D_3.

$$\frac{dw_1(\mathrm{x})}{dx} = \int_0^x \left[-\frac{1}{E_1 \cdot I_1 + E_2 \cdot I_2} \cdot \left(M_T(x) - \frac{b_2}{\lambda^2} \cdot \left[\frac{d\tau(x)}{dx} + m_1 \cdot \lambda^2 \cdot M_T(x) + \frac{1}{K_1} \cdot \frac{N_0}{E_2 \cdot A_2}\right] \cdot (y_1 + y_2 + t_a)\right) dx\right] + D3 \tag{94}$$

The equation of the vertical deformation in the reinforced zone of the beam is obtained by integrating the differential Eq. (93).

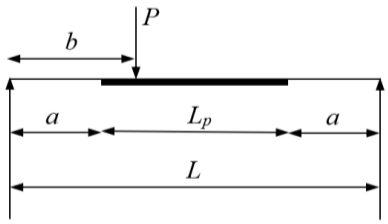

Fig. 2 Simply supported beam subjected to a concentrated load

$$w_1(x) = \int_0^x \left[\int_0^x \left[-\frac{1}{E_1 \cdot I_1 + E_2 \cdot I_2} \cdot \left(M_T(x) - \frac{b_2}{\lambda^2} \cdot \left[\frac{d\tau(x)}{dx} + m_1 \cdot \lambda^2 \cdot M_T(x) + \frac{1}{K_1} \cdot \frac{N_0}{E_2 \cdot A_2} \right] \cdot (y_1 + y_2 + t_a) \right) dx \right] + D3 \right] dx + D4 \quad (95)$$

Where D_4 is the integration constant.

The differential equation of the deformation of the unreinforced part of the beam is expressed using the Navier-Bernoulli hypothesis as follows

$$\frac{d^2 v_1(x)}{dx^2} = \frac{-M_T(x)}{E_1 \cdot I_1} \quad (96)$$

Integrating this equation twice, we obtain the expression for the vertical deformation in the unreinforced zone of the beam note $v_1(x)$

$$\frac{dv_1(x)}{dx} = \int_0^x \frac{-M_T(x)}{E_1 \cdot I_1} + D1 \quad (97)$$

$$\mathrm{v}_1(\mathrm{x}) = \int_0^x \left[\int_0^x \frac{-M_T(x)}{E_1 \cdot I_1} + D1 \right] dx + D2 \quad (98)$$

Where D_1 and D_2 are the integration constants of this equation. The expression for the vertical deformation of the reinforced beam is defined as follows

$$\omega(x) = V_1(x) + \omega_1(x) \cdot \big(u_2(x) - u_1(x)\big) \quad (99)$$

The integration constants D_1, D_2, D_3 and D_4 are determined by checking the appropriate boundary conditions. These conditions are expressed by the following expressions:

$v_1(x = -a) = 0, v_1(x = 0) = w_1(x = 0), \frac{dv_1}{dx}(x = 0) = \frac{dw_1}{dx}(x = 0)$ et $\frac{dw_1}{dx}\left(x = \frac{Lp}{2}\right)$

In the case of a simply supported beam subjected to a concentrated load (Fig. 2).

For a<b

$$\tau(x) = \begin{cases} B_3\, cosh(\lambda x) + B_4\, sinh(\lambda x) + m_1\, P\left(1 - \frac{b}{L}\right), & 0 \le x \le (b-a) \\ B_5\, cosh(\lambda x) + B_6\, sinh(\lambda x) - m_1\, P\frac{b}{L}, & (b-a) \le x \le L_p \end{cases} \quad (100)$$

For a>b

$$\tau(x) = B_7\, cosh(\lambda x) + B_8\, sinh(\lambda x) - m_1\, P\frac{b}{L} \quad 0 \le x \le L_p \quad (101)$$

Where P is the concentrated load and $k=\lambda\,(b\text{-}a)$, by applying the boundary conditions for this case and for both cases where $a>b$ and $a<b$, the constants B_3, B_4, B_5, B_6, B_7, and B_8 can be

Table 3.1 Geometric characteristic of the beam

Components	Width (mm)	Thickness (mm)	Young's module (MPa)	Poisson coefficient	Transverse shear modulus (MPa)
RC beam	200	300	30000	0.20	12500
Adhesive layer (RC beam)	200	2.0	2000	0.35	740
CFRP plate (bonded to RC beam)	200	4.0	100000	0.30	38460

determined as follows

$$B_3 = \frac{m_2 Pa}{\lambda}\left(1 - \frac{b}{L}\right) - m_1\, P e^{-k} - \xi \tag{102}$$

$$B_4 = -\frac{m_2 Pa}{\lambda}\left(1 - \frac{b}{L}\right) - \xi \tag{103}$$

$$B_5 = \frac{m_2 Pa}{\lambda}\left(1 - \frac{b}{L}\right) - m_1\, P\, sinh(k) - \xi = -B_6 \tag{104}$$

$$B_7 = \frac{m_2 Pa}{\lambda}\left(1 - \frac{b}{L}\right) - \xi = -B_8 \tag{105}$$

3. Results and discussion

In this study, a reinforced concrete beam is supported by two simple supports, with a length of three meters (3 m) (Fig. 1). This beam is subjected to a distributed load q=50 KN/m. The length of the strengthening plate is Lp=2.4 m, and the distance between the support and the plate is denoted by a (a=0.3 m). The dimensions of the reinforced beam section are summarized in Table 3.1.

In this section, we present the numerical results, in the form of tables and graphs, of the method outlined in this work. The influence of parameters such as geometric and mechanical properties, as well as the prestressing force of the plate, on the interfacial stresses and flexural behavior of the reinforced beam has been studied. The results obtained by this method have been compared to those in existing literature.

The high interfacial stresses, both normal and shear, at the ends of the plate could lead to premature detachment. Therefore, accurately and reliably determining these stresses can reduce the risk of failure of the reinforced beam without compromising the effectiveness of the strengthening technique. To this end, we have compared our analysis with other solutions in the literature (EL Amrani *et al.* (2006), Kerboua *et al.* (2011), Ghaafori *et al.* (2013) for beams reinforced with prestressed plates, and with Smith and Teng for non-prestressed plates.

Fig. 3 shows the interfacial shear stress variation along the prestressed plate's length, computed using both our method and the Al Amrani method, which excludes consideration of vertical loads on the reinforced beam. A reduction in the maximum shear stress is observed, especially at the end of the plate.

Fig. 4 illustrates the interfacial shear stresses of a beam reinforced by a non-prestressed plate subjected to a uniformly distributed load q=50 KN/m. The results were evaluated based on both the present method, Ghaafory *et al.* (2013), Smith and Teng (2001). The results obtained show good agreement among the three analytical studies. The Smith and Teng method is specifically

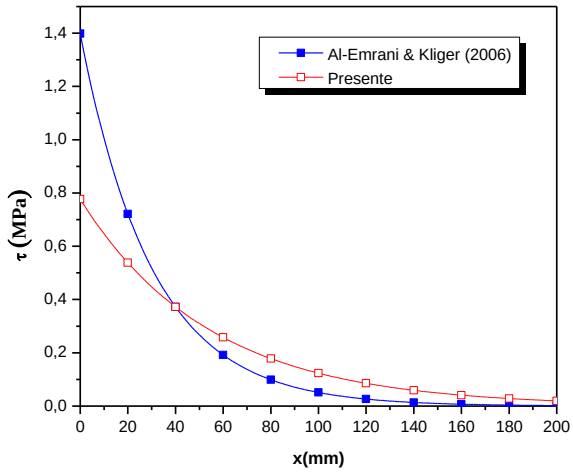

Fig. 3 Interfacial shear stresses for a reinforced beam with a prestressed bonded plate ($N0$=100 kN), without external load

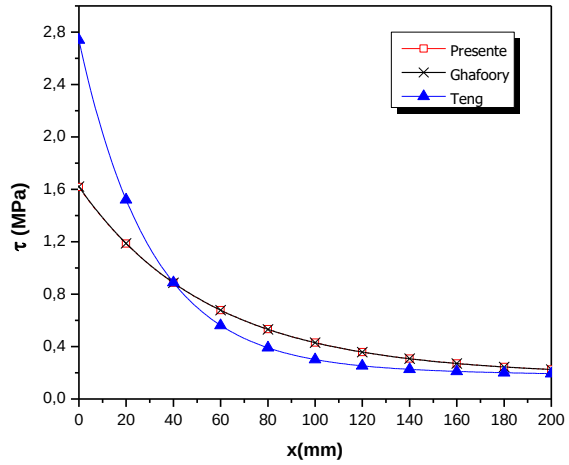

Fig. 4 Interfacial shear stresses for a reinforced beam with a non-prestressed bonded plate ($N0$=0 kN), with external load q=50 kN/m

designed for non-prestressed plates and does not account for shear-lag deformations. The two methods focus on calculating normal and shear interfacial stresses within the adhesive layer. The effect of prestressing on the overall flexural behavior of reinforced beams will be studied in this analysis.

Fig. 5 illustrates how shear deformations and increased prestressing force in the reinforcement plate affect shear interface stresses in the adhesive layer. The reinforced beam carries a load q (q=50 KN/m), while the plate experiences prestressing forces ranging from 0 to 50 KN.

Accounting for shear deformations significantly reduces the maximum stress at the plate's end by approximately 43.5% for a prestressing force of 50 KN. The shear effect becomes less significant for lower prestressing levels. Additionally, this figure shows that the maximum shear stress occurs at the plate's end and rises with increasing prestressing force. This stress diminishes

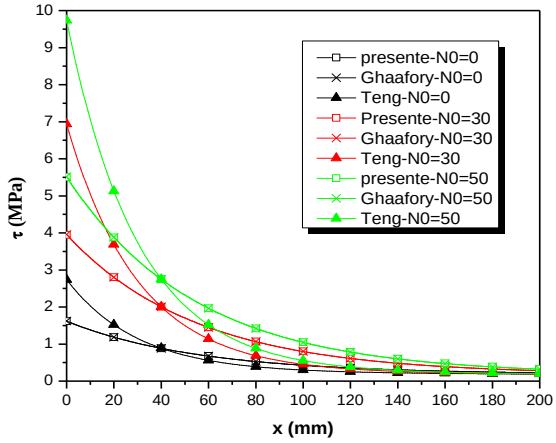

Fig. 5 Interfacial shear stresses for a reinforced beam for different values of the plate's prestressing force ($N0$=0, 30 KN and 50 KN), with external load q=50 kN/m

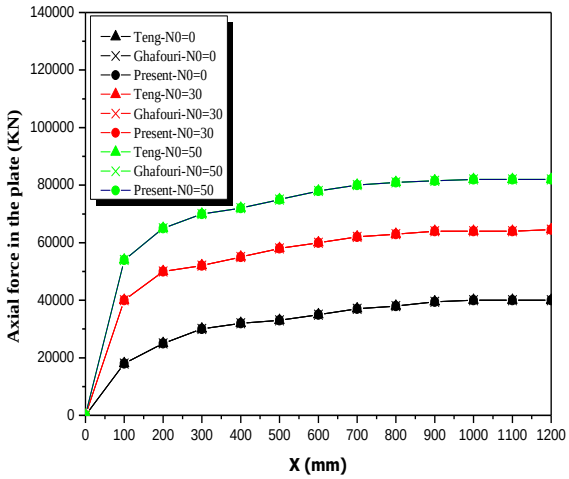

Fig. 6 Axial force as a function of the level of the prestressing force $N0$ and according to the length of the plate

rapidly, approaching very low values at distances of about 150 mm.

Fig. 6 shows that shear deformations do not alter the distribution of axial forces along the plate's length. However, these forces escalate swiftly from the plate's onset, explaining the elevated shear stress at the plate's end resulting from the load transfer between the beam and the reinforcing plate.

Fig. 7 illustrates the vertical deformation of the reinforced beam under a distributed load q=50 KN/m for various values of the plate's prestressing force ($N0$=0, 30, 50 KN). The left support of the reinforced beam is situated at a distance a=0.3 m from the origin of the x-axis, which is considered the left end of the plate. Despite the axial force and the distribution of interfacial shear stresses, the bending behavior of the plated beam remains unaffected by shear deformation. It is noted that as the prestressing force of the plate rises, the vertical deformation of the beam

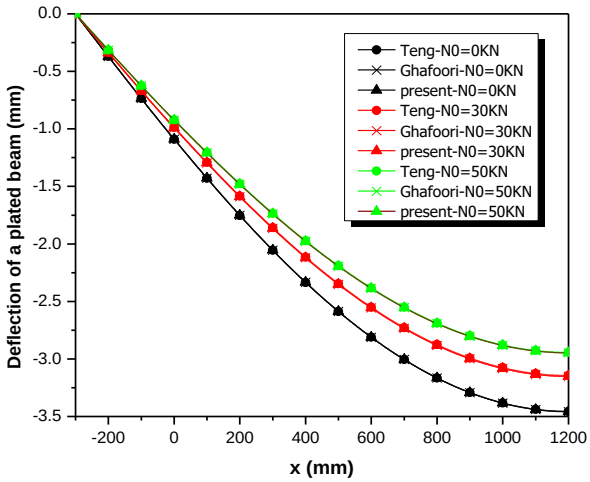

Fig. 7 Vertical deformation of the reinforced beam, with or without shear lag depending on the level of the prestressing force *N*0 of the reinforcing plate

decreases. This highlights the significance of considering prestressing in reducing deflection and enhancing the stiffness of the reinforced beam

4. Conclusions

This study examines the interfacial stresses and flexural behavior of reinforced concrete beams strengthened with prestressed FRP plates. The results demonstrate that prestressing significantly enhances flexural performance by increasing structural rigidity and reducing deformation, offering valuable insights for optimizing beam design in engineering practice.

These insights contribute significantly to advancing the understanding and optimization of reinforced beam structures in engineering applications.

While the current model employs linear elastic assumptions, future work should address material nonlinearities and complex stress distributions to enhance predictive accuracy. This extension would provide a more comprehensive understanding of structural behavior under realistic operating conditions.

References

Al-Emrani, M. and Kliger R. (2006), "Experimental and numerical investigation of the behaviour and strength of composite steel-CFRP members", *Adv. Struct. Eng.*, **9**(6), 819-831. https://doi.org/10.1260/136943306779369491.

Antar, K., Amara, Kh., Benyoucef, S., Bouazza, M. and Ellali, M. (2019), "Hygrothermal effects on the behavior of reinforced-concrete beams strengthened by bonded composite laminate plates", *Struct. Eng. Mech.*, **69**(3), 327-334. https://doi.org/10.12989/sem.2019.69.3.327.

Antar, K., Derbal, R. and Amara, Kh. (2024), "A study of thermal effects and strain gradient elasticity in wave propagation through matrix-embedded wall carbon nanotubes", *Vib. Eng. Technol.*, **12**, 8285-8295.

Barnes, R.A. and Mays, G.C. (2001), "The transfer of stress through a steel to concrete adhesive bond", *Int. J. Adhes.*, **21**(6), 495-502. https://doi.org/10.1016/S0143-7496(01)00031-8.

Beldjelili, Y., Tounsi, A. and Mahmoud, S.R. (2016), "Hygrothermo-mechanical bending of S-FGM plates resting on variable elastic foundations using a four-variable trigonometricplate theory", *Smart Struct. Syst.*, **18**(4), 755-786. https://doi.org/10.12989/sss.2016.18.4.755.

Benachour, A., Benyoucef, S., Tounsi, A. and Adda Bedia, E A. (2008), "Interfacial stress analysis of steel beams reinforced with bonded prestressed FRP plate", *J. Eng. Struct.*, **30**(11), 3305-3315. https://doi.org/10.1016/j.engstruct.2008.05.007.

Benchohra, M., Driz, H., Bakora, A., Tounsi, A., Adda Bedia, E.A. and Mahmoud, S.R. (2018), "A new quasi-3D sinusoidal shear deformation theory for functionally graded plates", *Struct. Eng. Mech.*, **65**(1), 19-31. https://doi.org/10.12989/sem.2018.65.1.019.

Benyoucef, S., Tounsi, A., Meftah, S.A. and Adda Bedia, E.A. (2006), "Approximate analysis of the interfacial stress concentrations in FRP-RC hybrid beams", *Compos. Interf.*, **13**(7), 561-571. https://doi.org/10.1163/156855406778440758.

Bouakaz, K., Hassaine Daouadji, T., Meftah, S.A., Ameur, M. and Adda Bedia, E.A. (2014), "A numerical analysis of steel beams strengthened with composite materials", *Mech. Compos. Mater.*, **50**(4), 685-696. https://doi.org/10.1007/s11029-014-9435-x.

Bouazaoui, L.A. (2008), "Analysis of steel/concrete interfacial shear stress by means of pullout test", *Int. J. Adhes.*, **28**(3), 101-108. https://doi.org/10.1016/j.ijadhadh.2007.02.006.

Bouderba, B., Houari, M.S.A. and Tounsi, A. (2013), "Thermomechanical bending response of FGM thick plates resting on Winkler-Pasternak elastic foundations", *Steel Compos. Struct.*, **14**(1), 85-104. https://doi.org/10.12989/scs.2013.14.1.085.

Bouhadra, A., Tounsi, A., Bousahla, A.A., Benyoucef, S. and Mahmoud, S.R. (2018), "Improved HSDT accounting for effect of thickness stretching in advanced composite plates", *Struct. Eng. Mech.*, **66**(1), 61-73. https://doi.org/10.12989/sem.2018.66.1.061.

Bourada, F., Amara, K., Bousahla, A.A., Tounsi, A. and Mahmoud, S.R. (2018), "A novel refined plate theory for stability analysis of hybrid and symmetric S-FGM plates", *Struct. Eng. Mech.*, **68**(6), 661-675. https://doi.org/10.12989/sem.2018.68.6.661.

Bousahla, A.A., Benyoucef, S., Tounsi, A. and Mahmoud, S.R. (2016), "On thermal stability of plates with functionally graded coefficient of thermal expansion", *Struct. Eng. Mech.*, **60**(2), 313-335. https://doi.org/10.12989/sem.2016.60.2.313.

Chikh, A., Tounsi, A., Hebali, H. and Mahmoud, S.R. (2017), "Thermal buckling analysis of cross-ply laminated plates using a simplified HSDT", *Smart Struct. Syst.*, **19**(3), 289-297. https://doi.org/10.12989/sss.2017.19.3.289.

Deng, J. and Marcus, M.K. (2004), "Stress analysis of steel beams reinforced with a bonded CFRP plate", *Compos. Struct.*, **65**(2), 205-215. https://doi.org/10.1016/j.compstruct.2003.10.017.

Elamary, A.S. and Abd-Elwahab, R.K. (2016), "Numerical simulation of concrete beams reinforced with composite GFRPSteel bars under three points bending", *Struct. Eng. Mech.*, **57**(5), 937-949. https://doi.org/10.12989/sem.2016.57.5.937.

El-Haina, F., Bakora, A., Bousahla, A.A., Tounsi, A. and Mahmoud, S.R. (2017), "A simple analytical approach for thermal buckling of thick functionally graded sandwich plates", *Struct. Eng. Mech.*, **63**(5), 585-595. https://doi.org/10.12989/sem.2017.63.5.585.

Ghafoori, E. (2013), "Interfacial stresses in beams strengthened with bonded prestressed plates", *Eng. Struct.*, **46**, 508-510. https://doi.org/10.1016/j.engstruct.2012.08.011.

Ghafoori, E. and Motavalli, M. (2013), "Flexural and interfacial behavior of metallic beams strengthened by prestressed bonded plates", *Compos. Struct.*, **101**, 22-34. https://doi.org/10.1016/j.compstruct.2013.01.021.

Gibson, R.F. (1994), *Principles of Composites Material Mechanics*, McGraw-Hill Inc.

Hadji, L., Hassaine Daouadji, T., Meziane, A.M. and Adda Bedia, E.A. (2016), "Analyze of the interfacial stress in reinforced concrete beams strengthened with externally bonded CFRP plate", *Steel Compos. Struct.*, **20**(2), 413-429. https://doi.org/10.12989/scs.2016.20.2.413.

Hassaine Daouadji, T. (2017), "Analytical and numerical modeling of interfacial stresses in beams bonded with a thin plate", *Adv. Comput. Des.*, **2**(1), 57-69. https://doi.org/10.12989/acd.2017.2.1.057.

Kerboua, B., Adda Bedia, E. and Benmoussat, A. (2011), "Strengthening of damaged structures with bonded prestressed FRP composites plates: An improved theoretical solution", *J. Compos. Mater.*, **45**(5), 499-512. https://doi.org/10.1177/0021998310387669.

Krour, B., Bernard, F. and Tounsi, A. (2014), "Fibers orientation optimization for concrete beam strengthened with a CFRP bonded plate: A coupled analytical-numerical investigation", *Eng. Struct.*, **56**, 218-227. https://doi.org/10.1016/j.engstruct.2013.05.008.

Malek, A.M., Saadatmanesh, H. and Ehsani, M.R. (1998), "Prediction of failure load of RC beams strengthened with FRP plate due to stress concentration at the plate end", *ACI Struct. J.*, **95**(1), 142-152. https://doi.org/10.14359/534.

Menasria, A., Bouhadra, A., Tounsi, A., Bousahla, A.A. and Mahmoud, S.R. (2017), "A new and simple HSDT for thermal stability analysis of FG sandwich plates", *Steel Compos. Struct.*, **25**(2), 157-175. https://doi.org/10.12989/sem.2017.25.2.157.

Roberts, T.M. (1989), "Approximate analysis of shear and normal stress concentrations in the adhesive layer of plated RC beams", *Struct. Eng.*, **67**(12), 229-233. https://doi.org/10.1016/j.commatsci.2009.01.020.

Roberts, T.M. and Haji-Kazemi, H. (1989), "Theoretical study of the behavior of reinforced concrete beams strengthened by externally bonded steel plates", *Proc. Inst. Civil Eng.*, **87**(2), 39- 55. https://doi.org/10.1680/iicep.1989.1452.

Robinovitch, O. and Frostig, Y. (2000), "Closed-form higher-order analysis of beams strengthened with FRP strips", *J. Compos. Constr.*, **4**(2), 65-74. https://doi.org/10.1061/(ASCE)1090-0268(2000)4:2(65).

Robinovitch, O. and Frostig, Y. (2001), "Nonlinear higher-order analysis of cracked RC beams strengthened with FRP strips", *J. Struct. Eng.*, **127**(4), 381-389. https://doi.org/10.1061/(ASCE)0733-9445(2001)127:4(381.

Smith, S.T. and Teng, J.G. (2001), "Interfacial stresses in plated beams", *Eng. Struct.*, **23**(7), 857-871. https://doi.org/10.1016/S0141-0296(00)00090-0.

Smith, S.T. and Teng, J.G. (2002), "FRP-strengthened RC beams. I: Review of debonding strength models", *Eng. Struct.*, **24**(4), 385-395. https://doi.org/10.1016/S0141-0296(01)00105-5.

Smith, S.T. and Teng, J.G. (2002), "FRP-strengthened RC beams. II: Assessment of debonding strength models", *Eng. Struct.*, **24**(4), 397-417. https://doi.org/10.1016/S0141-0296(01)00106-7.

Stratford, T. and Cadei, J. (2006), "Elastic analysis of adhesion stresses for the design of a strengthened plate bonded to a beam", *Constr. Build. Mater.*, **20**(1-2), 34-45. https://doi.org/10.1016/j.conbuildmat.2005.06.041.

Taljsten, B. (1997), "Strengthening of beams by plate bonding", *J. Mater. Civil Eng.*, **9**(4), 206-212. https://doi.org/10.1061/(ASCE)0899-1561(1997)9:4(206).

Touati, M., Tounsi, A. and Benguediab, M. (2015), "Effect of shear deformation on adhesive stresses in plated concrete beams: Analytical solutions", *Comput. Concrete*, **15**(3), 141-166. https://doi.org/10.12989/cac.2015.15.3.141.

Tounsi, A. (2006), "Improved theoretical solution for interfacial stresses in concrete beams strengthened with FRP plate", *Int. J. Solid. Struct.*, **43**(14-15), 4154-4174. https://doi.org/10.1016/j.ijsolstr.2005.03.074.

Tounsi, A. and Benyoucef, S. (2007), "Interfacial stresses in externally FRP-plated concrete beams", *Int. J. Adhes. Adhes.*, **27**(3), 207-215. https://doi.org/10.1016/j.ijadhadh.2006.01.009.

Vaddadi, P., Nakamura, T. and Singh, R.P. (2007), "Inverse analysis to determine hygrothermal properties in fiber reinforced composites", *J. Compos. Mater.*, **41**(3), 309-344. https://doi.org/10.1177/0021998306063372.

Vilnay, O. (1988), "The analysis of reinforced concrete beams strengthened by epoxy bonded steel plates", *Int. J. Cement Compos. Light Weight Concrete*, **10**(2), 73-78. https://doi.org/10.1016/0262-5075(88)90033-4.

Ye, J.Q. (2001), "Interfacial shear stress transfer of RC beams strengthened by bonded composite plates", *Cement Concrete Compos.*, **23**(4-5), 411-417. https://doi.org/10.1016/S0958-9465(01)00015-4.

Younsi, A., Tounsi, A., Zaoui, F.Z., Bousahla, A.A. and Mahmoud, S.R. (2018), "Novel quasi-3D and 2D

shear deformation theories for bending and free vibration analysis of FGM plates", *Geomech. Eng*., **14**(6), 519-532. https://doi.org/10.12989/gae.2018.14.6.519.

AP